

# Fluid Flow Induces Differential Detachment of Live and Dead Bacterial Cells from Nanostructured Surfaces

S. W. M. A. Ishantha Senevirathne, Yi-Chin Toh, and Prasad K. D. V. Yarlagadda\*

Cite This: *ACS Omega* 2022, 7, 23201–23212

Read Online

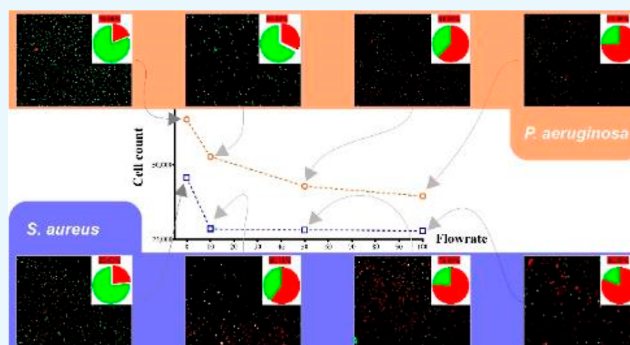
ACCESS |

Metrics &amp; More

Article Recommendations

Supporting Information

**ABSTRACT:** Nanotopographic surfaces are proven to be successful in killing bacterial cells upon contact. This non-chemical bactericidal property has paved an alternative way of fighting bacterial colonization and associated problems, especially the issue of bacteria evolving resistance against antibiotic and antiseptic agents. Recent advancements in nanotopographic bactericidal surfaces have made them suitable for many applications in medical and industrial sectors. The bactericidal effect of nanotopographic surfaces is classically studied under static conditions, but the actual potential applications do have fluid flow in them. In this study, we have studied how fluid flow can affect the adherence of bacterial cells on nanotopographic surfaces. Gram-positive and Gram-negative bacterial species were tested under varying fluid flow rates for their retention and viability after flow exposure. The total number of adherent cells for both species was reduced in the presence of flow, but there was no flowrate dependency. There was a significant reduction in the number of live cells remaining on nanotopographic surfaces with an increasing flowrate for both species. Conversely, we observed a flowrate-independent increase in the number of adherent dead cells. Our results indicated that the presence of flow differentially affected the adherent live and dead bacterial cells on nanotopographic surfaces. This could be because dead bacterial cells were physically pierced by the nano-features, whereas live cells adhered via physiochemical interactions with the surface. Therefore, fluid shear was insufficient to overcome adhesion forces between the surface and dead cells. Furthermore, hydrodynamic forces due to the flow can cause more planktonic and detached live cells to collide with nano-features on the surface, causing more cells to lyse. These results show that nanotopographic surfaces do not have self-cleaning ability as opposed to natural bactericidal nanotopographic surfaces, and nanotopographic surfaces tend to perform better under flow conditions. These findings are highly useful for developing and optimizing nanotopographic surfaces for medical and industrial applications.



## INTRODUCTION

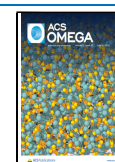
Discovery of the bactericidal effect of cicada and dragonfly wings lead to a new method of fighting bacterial colonization.<sup>1–4</sup> Nano-scale features, such as pillars, wires, and rods, fabricated on substrates exhibit a bactericidal effect similar to that of their natural counterparts.<sup>5</sup> Over the last decade, these bactericidal nanotopographic surfaces had a great progress, promising them to be the next generation of antibacterial surfaces. One of the biggest stakeholders of this emerging technology is the medical sector, which has higher hopes of applying these antibacterial surfaces on medical implants and devices, which have a greater risk of bacterial colonization. This risk is augmented by the increasing evolution of antimicrobial chemical-resistant strains. Several industries, such as food, aviation, and marine transport industries, are also impacted by bacterial colonization, and bactericidal nanotopographic surfaces have given an excellent opportunity for them to mitigate issues related to bacterial contamination. Research has been carried out to evaluate the suitability of this innovative technology for various sectors.

There are several different scientific explanations presented by researchers on the bacterial-killing mechanism of nanotopographic surfaces. Despite the differences in those theories,<sup>2,4,6</sup> all agreed that those cells are lysed by a physical mechanism but not by chemistry of the surface. The size and shape of nanofeatures have been shown to be influential in rupturing the bacterial membrane.<sup>7–10</sup> Consequently, the presence of any foreign material, such as dead bacteria on the nanofeatures, can compromise their bactericidal effectiveness. It has been reported that lysed bacterial cells remain on the nanotopographic surface,<sup>4</sup> and as a result, the nanofeatures may not be able to pierce subsequent bacterial cells as the tips are covered

Received: February 28, 2022

Accepted: June 15, 2022

Published: June 28, 2022



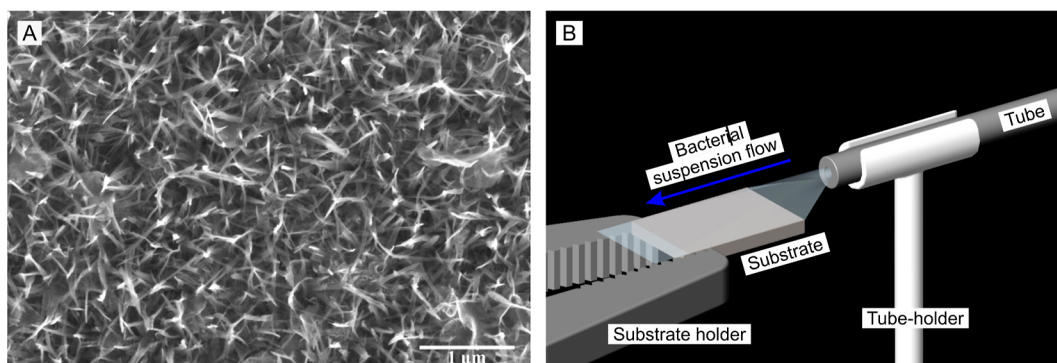


**Figure 1.** (A) Scanning electron microscopic image of the nano-wire structure fabricated on the Ti-6Al-4V substrate using the hydrothermal process with 1 M NaOH reacted at 180 °C for 3 h. The image was taken by field emission SEM (TESCAN MIRA 3) with 50,000 × magnification using 15 kV beam voltage at 8.04 mm working distance in a square area of 5.54 μm. (B) Experimental setup used for the experiment with the substrate held horizontally using a holder and the tube from the peristaltic pump directed toward the substrate. The substrate and the tube orifice were held on the same horizontal level allowing the bacterial suspension to freely flow over the substrate. The orifice had an internal diameter of 0.89 mm for 10 and 50 mL/min flow and 2.79 mm for 100 mL/min flow. The substrate was 7 mm wide, and therefore, fluid flow was well diverged on the substrate surface and sufficiently covered the entire surface area.

by pierced cells in the absence of flow that could remove these from the surface.<sup>11,12</sup> Since their inception, artificial bactericidal nanostructured surfaces have been through a vast development expanding into different structures and materials,<sup>13,14</sup> functionalizing nanostructured surfaces,<sup>15</sup> and killing viruses.<sup>16</sup>

There are ample examples showing that nanotopographic structures made on different substrates, such as titanium,<sup>17</sup> silicon,<sup>8</sup> aluminium,<sup>18</sup> and polymers,<sup>19</sup> have bactericidal effects. Various nanostructured surfaces have shown bactericidal efficacies above 85%.<sup>5,17,19–21</sup> Surfaces that are successful against bacterial species which are problematic in medical and industrial sectors are being developed.<sup>5,13</sup> This has laid a foundation for a promising mitigation method for bacterium-related issues and a potential candidate mechanism for chemical methods which are susceptible to being ineffective due to bacterial evolution. However, the bactericidal efficacy of these surfaces is mostly evaluated according to standardized testing methodologies, such as the ISO 22916:2011,<sup>22</sup> where bacterial incubation is performed under static conditions.<sup>12</sup> However, bactericidal nanotopographic surfaces are deployable in various industrial sectors, ranging from the medical to marine industry, whereby they are subjected to fluid flow conditions. Bacterial activities in static and dynamic fluid environments have been shown to be drastically different. Bacterial motion,<sup>23–26</sup> growth,<sup>27</sup> phenotyping,<sup>28</sup> adhesion and retention on solid surfaces,<sup>29–31</sup> and biofilm formation<sup>32</sup> have been shown to be affected by fluid flow conditions. Bacterial cells can get detached from the adherent surface under hydrodynamic forces.<sup>33,34</sup> By applying sufficient magnitude of force, bacterial cells can be detached from nanostructured surfaces as well.<sup>31</sup> Hence, bactericidal performance results obtained under static testing conditions may not be accurately extrapolated to dynamic environments. This warrants a need to study bacterial attachment, detachment, and viability on nanostructured surfaces under flow conditions for further developing these surfaces toward a successful realistic application.

Removal of bacteria from surfaces has been an interesting research question for a long time as it can help develop mitigation methods for surface decontamination and prevent biofilm formation. In this quest, detachment of bacterial cells

from various surfaces has been studied.<sup>35–38</sup> Numerous studies reported that fluid flow can detach adherent bacterial cells from smooth non-textured surfaces.<sup>29,36,39–41</sup> However, adhesion and detachment of bacteria from nanostructured surfaces are less understood.<sup>12</sup> The adhesion forces between bacterial cells and nanostructured surfaces have been shown to be reduced by the fluid flow, unlike on flat surfaces.<sup>29,42</sup> This could be due to the differences in the adhesion mechanism. Unlike smooth surfaces, cell adhesion for live and dead cells is mediated by different physical phenomena on nanotopographic surfaces. Due to the physical bactericidal mechanism, dead cells are pierced by the nanotopographic features on the surface.<sup>1,8,43</sup> On the other hand, live cells adhere to the surface by means of physiochemical interactions.<sup>44–46</sup> Hence, it is valid to hypothesize that live and dead cells have different magnitudes of adhesion forces with the nanotopographic surface, and fluid flow is likely to result in differential detachment of live and dead cells from nanotopographic surfaces. This raises questions on the effectiveness of nanotopographic surfaces under flow conditions and their ability for self-cleaning like their natural counterparts.

In this study, we have studied detachment of live and dead bacterial cells from nanotopographic surfaces under flow conditions. One Gram-positive species and one Gram-negative species of bacteria were incubated on the surface and exposed to a fluid flow over the surface with three different flowrates. A nanotopographic surface not subjected to flow and an untreated surface of the same material in the same size subjected to flow are used as the control experiment.

## ■ MATERIALS AND METHODOLOGY

### Maintenance and Incubation of Bacterial Cells.

Preparation of a bacterial suspension for incubation on sample substrates was adopted from the literature.<sup>47–50</sup> Colonies of *Staphylococcus aureus* (ATCC 25923) or *Pseudomonas aeruginosa* (ATCC 27853) were incubated in 5 ml of nutrient broth (Sigma-Aldrich, NutriSelect) in a shaking incubator at 37 °C and 220 RPM for 16 h. After incubation, this suspension was centrifuged at 5250g for 5 min, and the separated pellet was resuspended in 1× phosphate buffered saline (PBS). The suspension was adjusted to OD<sub>600</sub> 1.1 ± 0.1 for *S. aureus* and OD<sub>600</sub> 0.5 ± 0.1 for *P. aeruginosa*.

**Preparation of Substrates.** Two sets of titanium (Ti-6Al-4V Grade-5) substrates sized  $7 \times 10$  mm were used for the experiments. This chosen nanowire structure fabricated with a hydrothermal process on a Ti-6Al-4V alloy has been extensively studied by previous researchers for antibacterial property<sup>51,52</sup> and eukaryotic cell proliferation.<sup>53</sup> The set of substrates that have undergone the hydrothermal synthesis process is referred to as treated substrates in this report. Prior to the hydrothermal process, the substrates were polished to 0.04  $\mu\text{mRa}$  surface roughness using electro polishing. Substrates were reacted in 1.0 M sodium hydroxide (NaOH) at 180 °C for 2 h to form the nanowire structure.<sup>51,54</sup> This set of fabrication parameters results in a nanowire structure on the titanium substrate with an average wire diameter of 50 nm and a height of 300 nm,<sup>51</sup> and the modified surface was hydrophilic.<sup>53</sup> Images taken using a field emission scanning electron microscope (TESCAN Mira 3) were used to confirm the nanostructure formation on the substrates. Polished substrates without hydrothermal treatment were the second type of substrate used for the experiment which are referred to as untreated substrates. Nanostructured or polished substrates were soaked in 80% ethanol for 15 min and washed with a stream of sterile PBS and exposed to UV light for 20 min, before incubating bacterial cells on them.

**Cell Detachment under the Flow Experiment.** Treated and untreated substrates were placed in a 24-microwell plate, and 500  $\mu\text{L}$  of the turbidity-adjusted bacterial suspension was pipetted in to the microwell. The cells were allowed to incubate on the substrate for 2 h. Afterward, the substrates were rinsed with sterile PBS at a prescribed flowrate for 2 min. Three rinsing flowrates (10, 50, and 100 mL/min) were evaluated using a peristaltic pump (Ismatec ISM915A with a CA-12 cassette) with  $\varnothing$  0.89 mm isoprene tubing for 10 and 50 mL/min flowrates and  $\varnothing$  2.79 mm tubing for the 100 mL/min flowrate. The open end of the tube was placed at one end of the substrate allowing the fluid to flow freely over the substrate as illustrated in Figure 1B. An open flow was used to rinse the substrate to prevent stagnation, trapping, and recirculation of detached cells. All experiments were repeated three times. Three controls were used in this experiment: a set of treated and untreated surfaces without rinsing and three untreated surfaces rinsed with the three tested flowrates. The two samples that were not rinsed are referred to as static non-rinsed samples. Levels of dependent and controlled variables are presented in Table 1A. The Reynolds number for the flow was calculated using eq 1 with  $\rho = 997 \text{ kg}\cdot\text{m}^{-3}$  and  $\mu = 0.00102 \text{ Pa}\cdot\text{s}$ . Linear velocity ( $u$ ) was calculated with the flowrate ( $Q$ ) and cross-sectional area ( $A$ ) by using eq 2.

$$\text{Re} = \rho \cdot u \cdot d_h / \mu \quad (1)$$

$$u = \frac{Q}{A} \quad (2)$$

**Cell Concentration Varying Experiment.** An experiment was designed to test if the number of dead cells on the nanostructured substrate varies with varying inoculum concentrations. The bacterial suspension was prepared in eight different concentrations measured by turbidity, and eight separate substrates were exposed to 1 mL of each bacterial suspension of *S. aureus* for 20 min. Then, the substrates were removed from the suspension and stained with a fluorescence dye. After staining for 15 min, cells were fixed using

**Table 1. Dependent and Controlled Variables for (A) Cell Detachment Experiment and (B) Cell Concentration Varying Experiment**

(A) cell detachment experiment	
bacterial species	<i>P. aeruginosa</i> <i>S. aureus</i>
surfaces	treated (nanowire-structured) surface untreated surface
bacterial cell concentration ( $\text{OD}_{600}$ )	$0.5 \pm 0.1$ for <i>P. aeruginosa</i> $1.1 \pm 0.1$ for <i>S. aureus</i>
rinsing flowrates (mL/min)/Reynolds number for the flow	0 (No flow) 10/237 50/1,186 100/757
flow duration (minutes)	2
(B) cell concentration experiment	
bacterial species	<i>S. aureus</i>
surfaces	treated (nanowire-structured) surface
bacterial cell concentration ( $\text{OD}_{600}$ )	$\times 8$
flow condition	static (no flow)
incubation period (minutes)	20

paraformaldehyde and taken for imaging. The experiment was repeated three times. The number of live and dead cells was quantified on the basis of surface coverage. 20 images of each substrate [ $10 \times (\text{live} + \text{dead})$ ] were taken. Table 1 (B) shows the values of variables used in the experiment.

**Fluorescence Staining and Imaging.** 3  $\mu\text{L}$  of the LIVE/DEAD BacLight Kit (Invitrogen detection technologies, L7012) mixture containing a 1:1 ratio mix of SYTO9 and propidium iodide (PI) made by diluting 5  $\mu\text{L}$  of each component in 1 mL of PBS was pipetted onto each substrate and allowed to incubate and dry for 15 min. Stained substrates were imaged using a Nikon Eclipse TiS inverted microscope with FITC and CY3 filter cubes. The field of view (FoV) of images was  $206.40 \times 165.12 \mu\text{m}$ . Each sample was randomly imaged 15 times each with the FITC filter and CY3 filter, resulting in 15 live-stained and 15 dead-stained images for each sample. Each experiment is repeated three times, and hence, at least 45 data points were obtained for each condition.

**Postprocessing of Images and Cell Enumeration.** Fluorescence images were color-balanced and binarized, before counting the pixels above threshold brightness. Images were taken with  $1280 \times 1280$  pixel resolution with a  $206.40 \times 165.12 \mu\text{m}$  FoV. The number of pixels above threshold brightness is interpreted as a quantification of cells on the substrates. Images were color-balanced and binarized using ImageJ software. Biofilm Analyzer software<sup>55</sup> was used to count the number of pixels illuminated after thresholding (with ImageJ). Instead of counting the individual cells, the number of illuminated pixels was used as a representative count of cells either dead or live. One pixel above the threshold illuminance in an area of  $511,211 \mu\text{m}^2$  (equal to the area covered by 15 images) was defined as a unit of bacterial cells and was used to quantify the adherent bacterial cells. Alternatively, a cell count could be calculated by dividing the total number of pixels by average pixel size of an individual cell. However, bacterial cells differ largely in size, and hence, this can result in errors in cell number calculations. Automatic cell counting was not used due to the variations in bacterial cell size and deviation of cells from

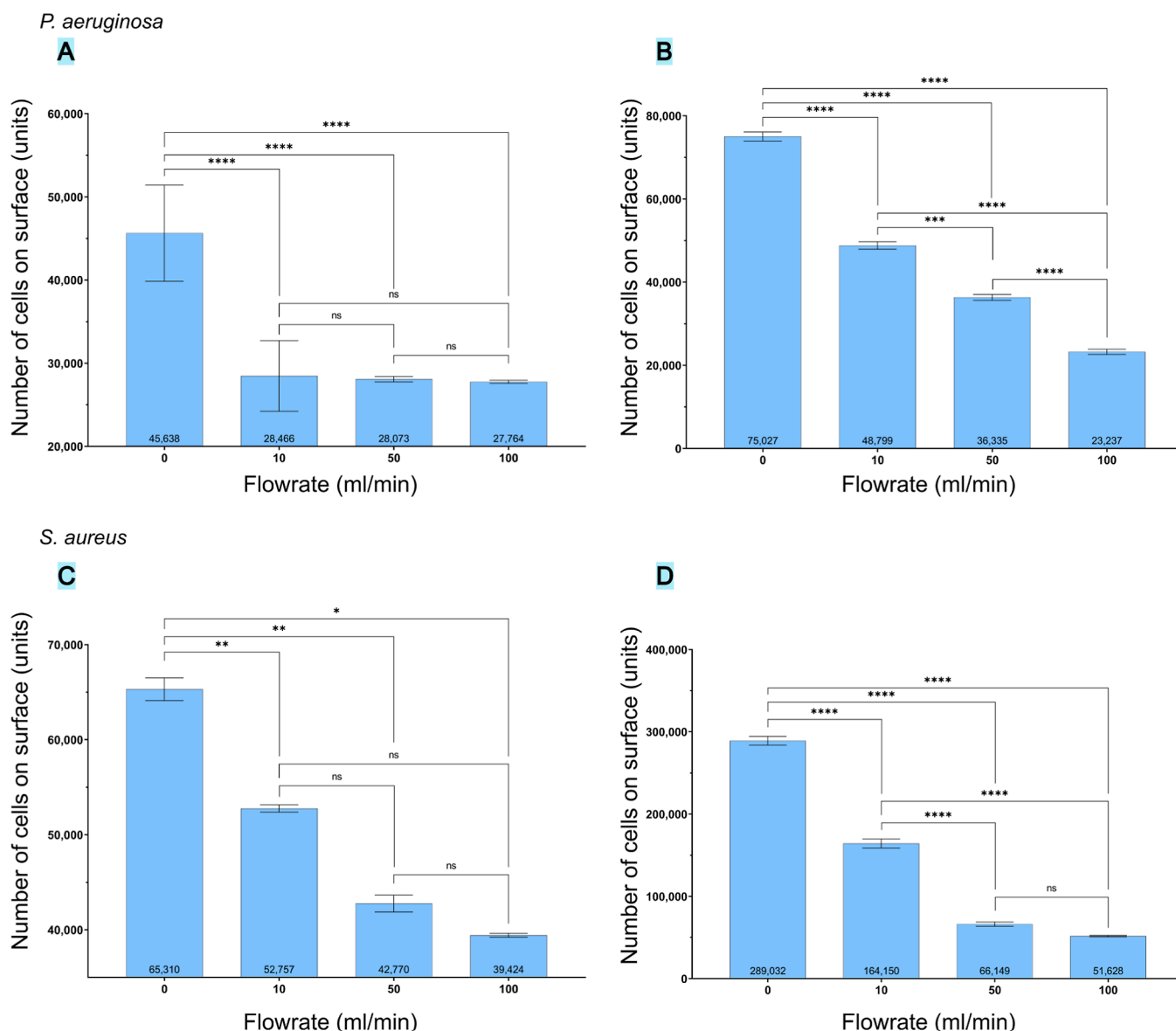


**Figure 2.** Adherent cell counts on treated and untreated surfaces under different flow conditions. (A) *P. aeruginosa* on the treated surface. (B) *P. aeruginosa* on the untreated surface. (C) *S. aureus* on the treated surface. (D) *S. aureus* on the untreated surface. Graphs show the mean cell count  $\pm$  SEoM of 45 data points from three independent experiments. Bacterial cells were incubated on substrates for 1 h and rinsed using a stream of sterile PBS with a specified flowrate (except the no flow) and stained with SYTO9 and PI before imaging using a fluorescence microscope. The adherent cell number was quantified using pixel counting on binarized fluorescence images. The unit defined as 1 pixel (on the binarized image) per an area of  $\sim 5 \times 10^6 \mu\text{m}^2$  on the surface. \* shows statistical significance with ANOVA. ns:  $P > 0.05$ , \*:  $P \leq 0.05$ , \*\*:  $P \leq 0.01$ , \*\*\*:  $P \leq 0.001$ , and \*\*\*\*:  $P \leq 0.0001$ .

typical shapes. In addition, the clustering of cells together makes it difficult for the software tools to identify cells due to ambiguity of cell boundary demarcation. For the same reason and because of the time consumption due to the substantial number of images required to be processed, manual cell counting was not used. Post-processed live-stained and dead-stained images were merged using ImageJ software for qualitative assessment of the cell viability on the surfaces.

**SEM Imaging of Biological Samples.** Field emission gun scanning electron microscopy was used to image bacterial cells on the substrates following the rinsing flow. Immediately following the flow cycle, cells were fixed and dehydrated before coating with a 10 nm gold layer for imaging. Without additional rinsing, the substrate was immersed in 2.5% glutaraldehyde in PBS. Then, it was incubated at room

temperature for 15 min. Then, substrates were retrieved and re-immersed in PBS overnight. Sample dehydration was done by different ethanol concentrations, 30, 50, 70, 80, 90, and 100%. Samples were incubated for 10 min in each ethanol concentration, except for 100% ethanol, in which the incubation is done for 1 h. Then, the substrates were stuck onto SEM stubs and coated with a 10 nm-thick layer of gold.

**Statistical Analysis.** Analysis of variance (ANOVA) was used to assess the significance of differences in group mean values between the groups using GraphPad Prism software. A confidence interval of 95% was used with  $p \leq 0.05$  taken as statistically significant. Statistical significance with ANOVA is shown by ns:  $P > 0.05$ , \*:  $P \leq 0.05$ , \*\*:  $P \leq 0.01$ , \*\*\*:  $P \leq 0.001$ , and \*\*\*\*:  $P \leq 0.0001$ .

## RESULTS

SEM images of the fabricated substrates are shown in Figure 1A showing the nanowire structure fabricated by the hydrothermal synthesis process.

**Flow-Induced Cell Detachment from Nanostructured Surfaces.** The total number of adherent cells (live and dead) remaining on the treated and on untreated surfaces with different flow conditions is shown in Figure 2. The graph shows the mean number of cells (in units) that remained on the surface  $\pm$  standard error of mean (SEoM). The adherent cell count from no-flow conditions to flow conditions was significantly reduced for both *P. aeruginosa* and *S. aureus* species. While the adherent cell count on the untreated surface was flowrate-dependent, the cell count on the treated surface was not flow-dependent. Although there is a reduction in the number of cells with the increasing flowrate, the differences were statistically insignificant. As shown in Figure 2, the mean adherent cell count of *P. aeruginosa* on the treated surface dropped from  $45,638 \pm 4,279$  at no flow to  $28,466 \pm 1,482$ ,  $28,073 \pm 796$ , and  $27,764 \pm 802$  units with 10, 50, and 100 mL/min flowrates, respectively, but the differences of means of three flowrates were not significant. In contrast, the cell count on the untreated surface was significantly reduced except between 50 and 100 mL/min flowrates. It was dropped from  $75,027 \pm 1,835$  at no flow to  $48,799 \pm 1,936$ , to  $36,335 \pm 1,427$ , and to  $23,237 \pm 1,157$  cells with 10, 50, and 100 mL/min flowrates, respectively. Similarly, *S. aureus* on the treated surface had significant reduction in the cell count from no-flow to flow conditions, but the differences of the cell count between flowrates were statistically insignificant. The cell count was reduced from  $65,310 \pm 932$  at no flow to  $52,757 \pm 819$ ,  $42,770 \pm 506$ , and  $39,424 \pm 1,262$  units with 10, 50, and 100 mL/min flowrates, respectively. The same trend with *P. aeruginosa* and *S. aureus* was observed on the untreated surface with significant reduction in the cell count from no flow to flow and between flows except 50 and 100 mL/min. The cell count at no flow was  $289,032 \pm 12,201$ , and it was dropped to  $164,150 \pm 7,780$ ,  $66,149 \pm 3,804$ , and  $51,628 \pm 2,171$  units of cells with three flowrates in the ascending order.

The tested lowest flowrate of 10 mL/min caused a reduction in the *P. aeruginosa* cell count on the treated surface from  $45,638 \pm 4,279$  at no flow to  $28,466 \pm 1,482$  at 10 mL/min, which is 39% while that of *S. aureus* was from  $65,310 \pm 932$  to  $52,757 \pm 819$  which is only a 19% drop. In comparison, on the untreated surface, *P. aeruginosa* was reduced from  $75,027 \pm 1,835$  to  $48,799 \pm 1,936$  which is about 35%, and the same reduction with *S. aureus* was observed from  $289,032 \pm 12,201$  to  $164,150 \pm 7,780$  which is a 43% drop. However, *S. aureus* had higher adhesion on the treated surface under no flow of  $65,310 \pm 932$  compared to  $45,638 \pm 4,279$  of *P. aeruginosa*. On the untreated surface, the same trend was observed with  $289,032 \pm 12,201$  for *S. aureus* and  $75,027 \pm 1,835$  for *P. aeruginosa* species.

**Live to Dead Cell Ratio Decreases with Flow.** The fluorescence images shown in Figure 3 show the number of cells under flow conditions on treated and untreated surfaces. On the treated surface for both species, it was evident that the proportion of live cells decreases with the increasing flowrate. However, untreated surfaces did not show such a trend with the increasing flowrate. Reduction of the total cell count was apparent on both types of surfaces, but the live/dead cell ratio on the untreated surface was not reduced compared to that on

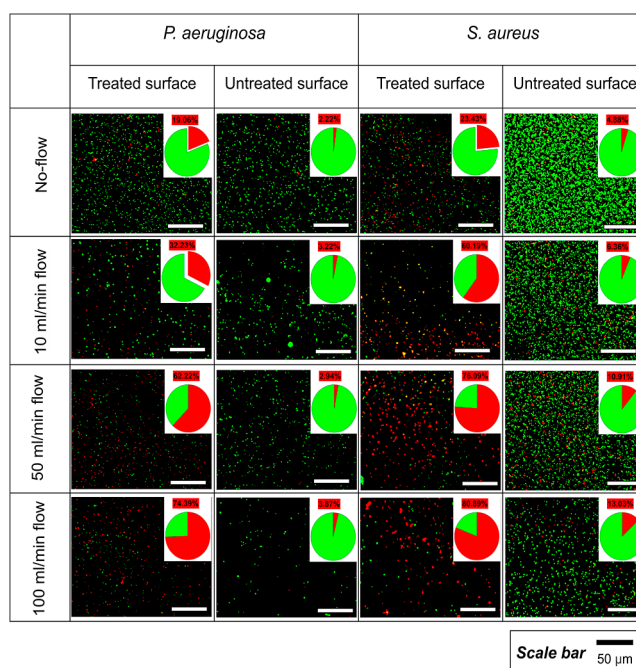


**Figure 3.** Fluorescence images of *P. aeruginosa* (left) and *S. aureus* (right) species on treated and untreated surfaces under the four flow conditions tested. Bacterial cells were incubated on the surface and rinsed with a 10, 50, and 100 mL/min stream of sterile PBS, while no flow was done on two sets of surfaces. The treated surface has a nanowire structure fabricated on it using the hydrothermal synthesis process on the smooth surface, while the untreated surface has smooth surfaces without undergoing hydrothermal synthesis. Live cells are green in color, and dead cells are red in color. Images are taken by staining cells with SYTO9 and PI and imaged using FITC and CY3 filters. The number of adhered cells was quantified using a unit defined as 1 pixel (above the threshold level on the binarized image) on an area of  $\sim 5 \times 10^6 \mu\text{m}^2$  on the surface.

the treated surface. Compared to the untreated surface, a higher number of dead cells were observed on the treated surface, confirming the bactericidal effect of the nanowire-structured surface as reported in previous studies.<sup>53</sup> The dead cell percentage of *P. aeruginosa* on the treated surface was increased from 19% at no flow to 32, 62, and 74% on three flowrates. In contrast to this, on the untreated surface, irrespective of the flow condition, the dead cell percentage varied between 2 and 4%. Similarly, with *S. aureus*, the dead cell percentage was 23% under the no-flow condition and increased to 60, 76, and 81% with the three flowrates. However, unlike *P. aeruginosa* on the untreated surface, *S. aureus* on the same surface was increasing with the flowrate. 5% dead cells under the no-flow condition were increased to 6, 11, and 13% with the three flowrates.

**Bacterial Cell Morphology after Rinsing.** SEM images were used for a qualitative analysis of the cell morphology of remaining cells on treated and untreated surfaces. Figure 4 presents the SEM images of the two species with and without rinsing the surfaces. Figure 4A shows an image of *P. aeruginosa* on the untreated flat polished surface with no nanowires on it. The cells appeared to be healthy as they were able to retain their cell morphology. This was drastically different on treated surfaces. Figure 4B–D shows images of *S. aureus*, and Figure 4E and F shows images of *P. aeruginosa* cells after rinsing. A flat cell morphology suggests that the cell has been lysed, and

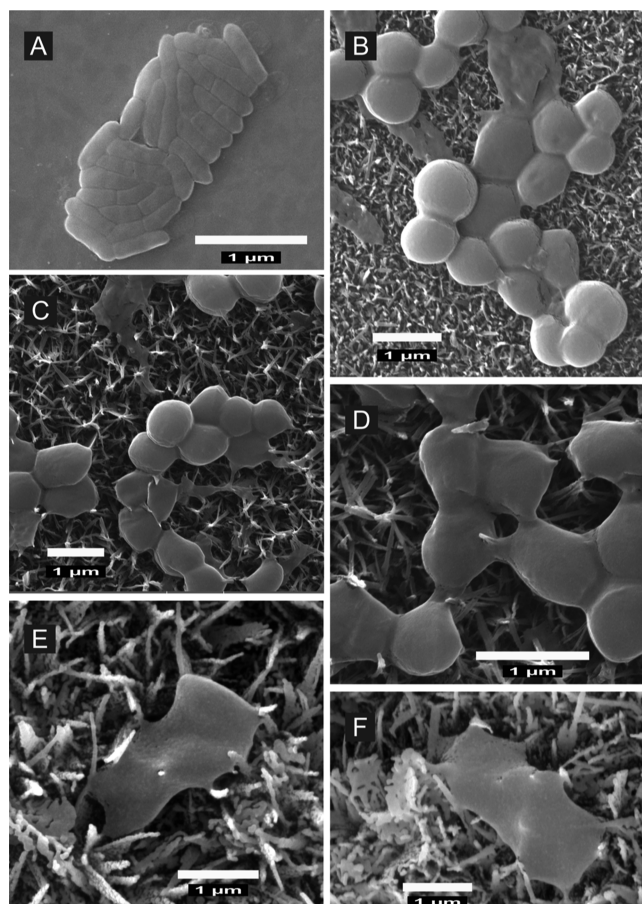


**Figure 4.** Scanning electron microscope images of bacterial cells on nanostructured and flat surfaces. Cells were fixed using 2.5% glutaraldehyde and dehydrated using ethanol before being coated with a 5 nm layer of gold. (A) *P. aeruginosa* cells on the untreated smooth titanium surface (no nanowires). (B) *S. aureus* cells on the treated titanium surface (with nanowires) without rinsing. (C,D) *S. aureus* cells on the treated surface after being rinsed with PBS at a 100 mL/min flowrate for 2 min. (E,F) *P. aeruginosa* cells on the treated surface after being rinsed with PBS at a 100 mL/min flowrate for 2 min.

notably, it can be observed that nanowires have pierced through some of those flat cells. Cells getting pierced by nanoscale features under static conditions have been reported previously,<sup>8</sup> and it has been argued that the flow can cause more cell lysing due to potential collisions with nanofeatures under flow.<sup>11</sup>

**Dead Cell Count on Nanostructured Surfaces Increases with Flow.** Figure 5 shows the number of live and dead cells (mean cell count  $\pm$  SEoM) on the two types of surfaces under different flow conditions. The dead cell count on the treated surface for both *P. aeruginosa* and *S. aureus* showed an increase from no flow to flow, while the live cell count was reduced from no flow to flow. On the contrary, on the untreated surface, the dead cell count decreased with the increasing flowrate, but the differences were statistically insignificant. The live cell count on the untreated surface for both species was significantly decreased with the increasing flowrate.

Live cells of *P. aeruginosa* were reduced by the flow, and the number of live cells remaining after the flow was flowrate-dependent on both treated and untreated surfaces. On the

untreated surface, there was no significant difference in the dead cell count with the flow. However, on the treated surface, the number of dead cells was not increased from no flow to 10 mL/min flow, but the dead cell count increased from 10 mL/min flow to 50 mL/min flow, and no significant difference between 50 and 100 mL/min flows was observed. Live *S. aureus* cells detached from the untreated surface with significant reduction in the cell count, except between 50 and 100 mL/min flows. Fluid flow caused the live cells to detach from the treated surface, but the differences of the cell count between three flowrates were insignificant. The dead cell count on the untreated surface had no significant effect from the fluid flow, but the flow caused a significant cell detachment from the treated surface without any dependency on the flowrate.

**Nanostructured Surface Can Lyse a Limited Number of Cells.** The number of live and dead *S. aureus* cells (mean  $\pm$  SEoM) on the treated surface with the increasing inoculum cell population under static conditions is shown in Figure 6A. The increasing bacterial inoculum concentration resulted in the increasing number of adherent cells on the nanostructured surface. Although the number of adherent cells increased, the number of dead cells initially increased and thereafter was observed to be asymptotic with the increasing inoculum concentration. At cell concentrations below OD<sub>600</sub> 0.1100, both live and dead cell numbers on the surface increased with the increasing cell concentration. Above this concentration, the number of dead cells on the surface remained unchanged, while the live cell count increased along with the cell concentration. Figure 6B and C shows the SEM images of substrates with lowest (OD<sub>600</sub> = 0.0022) and highest (OD<sub>600</sub> = 0.5038) inoculum concentrations. Lysed bacterial cells can be identified from their flat morphology, while viable cells remained in their original coccus shape. An interesting observation was that viable cells were observed to be on top of lysed cells. This suggests that contact with nanowires causes cells to lyse, and cell lysing ability of the nanowires gets hindered when contact between the nanowire and cell has been obstructed.

## DISCUSSION

Trends of bacterial cell detachment under flow for *S. aureus* and *P. aeruginosa* species were comparable to each other. The flow-induced detachment of *P. aeruginosa* cells from the nanotopographic surface was observed, but the increasing flowrate did not increase the detachment of cells. However, the *S. aureus* cell count was decreased with the increasing flowrate, but the differences were statistically insignificant. This effect is distinctive on the nanostructured surface as the untreated control sample had a decreased cell count for both species with the increasing flowrate. Despite both substrates being made of the same material, the nanostructure had masked the effect of flow on cells and therefore prevented them from getting removed from the surface. Nevertheless, the total cell adhesion of *P. aeruginosa* and *S. aureus* on the treated surface under all conditions was less than that on the untreated surface. Cell adhesions for *P. aeruginosa* were  $45,638 \pm 4,279$  and  $75,027 \pm 1,835$  units, while for *S. aureus*, they were  $65,310 \pm 932$  and  $289,032 \pm 12,201$  units on treated and untreated surfaces, respectively. Altogether, nanostructures on the surface can reduce bacterial adhesion, which has been previously reported. Since the cell incubation in this experiment was done under static conditions (no flow), the results of the no-flow

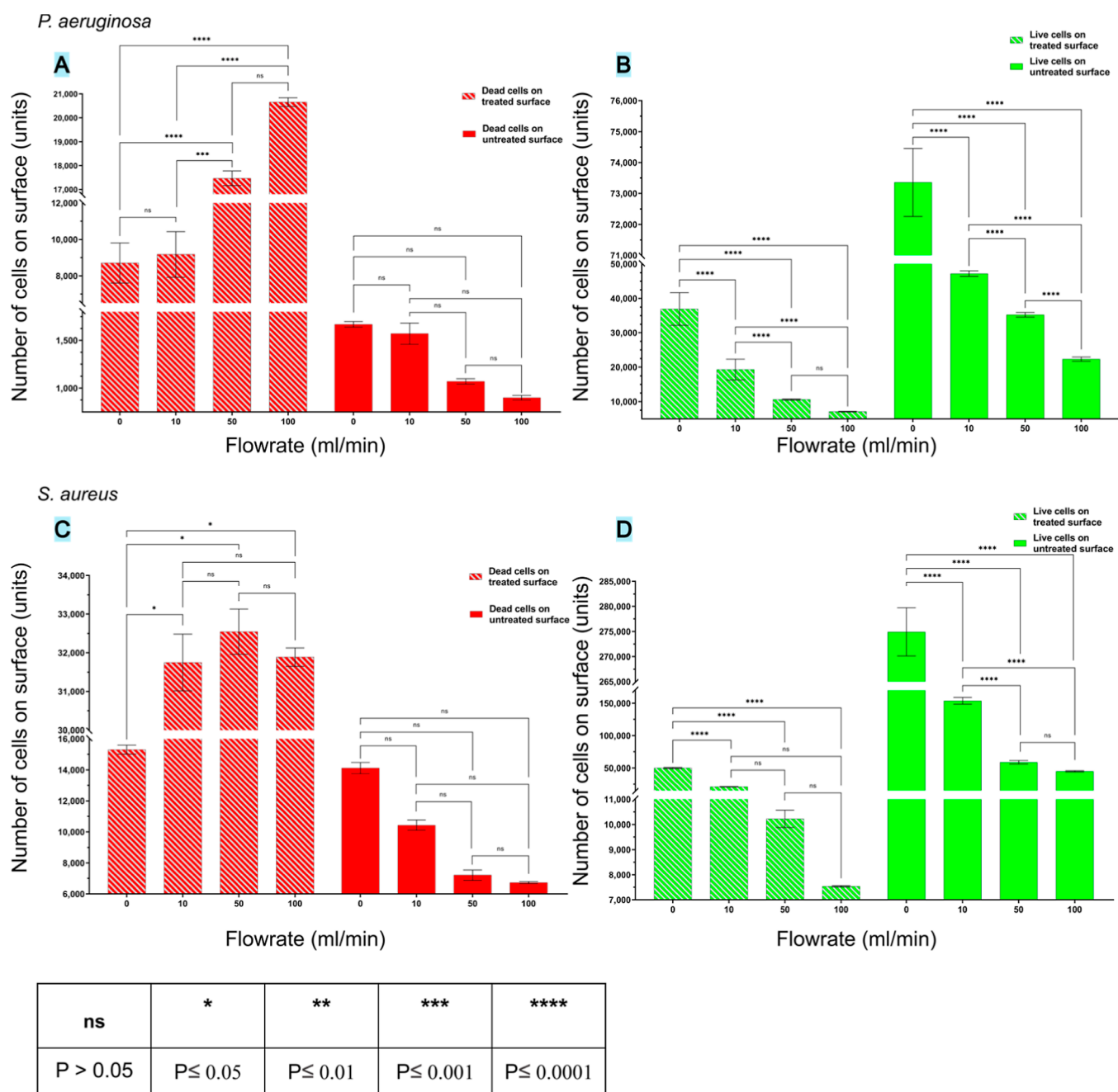


**Figure 5.** Number of live and dead cells on treated and untreated surfaces under different flow conditions. Following incubation and rinsing, the cells were stained with a mixture of SYTO9 and PI. Then, the cells were imaged using a fluorescence microscope with FITC and CY3 filters. Cells were quantified by counting pixels of each image above the threshold level. (A,B) shows dead and live *P. aeruginosa* cell counts, respectively. (C,D) shows the cell counts of *S. aureus* dead and live, respectively. Data are the mean of 45 images of three independent experiments  $\pm$  standard error of means. \* shows statistical significance with Student's *t*-test. ns:  $P > 0.05$ , \*:  $P \leq 0.05$ , \*\*:  $P \leq 0.01$ , \*\*\*:  $P \leq 0.001$ , and \*\*\*\*:  $P \leq 0.0001$ .

experiment can be compared with those of cell attachment experiments in the literature, and the results agree. Although the adherent cell count did not significantly vary with the flowrate, proportions of live and dead cells within the total adherent cells were varied on the nanostructured surface. The reduction in the total cell count from no-flow to flow conditions shows that due to the flow, a certain number of cells are being removed from the surface. However, there is no significant variation in the adherent cell count between the three flowrates. This indicates that the cell detachment from the nanostructured surface is not flowrate-dependent. Nevertheless, viability of the removed cells could not be directly

determined. Significant reduction in the remaining live cell count suggests that due to the flow, live cells are getting removed from the nanostructured surface. Decrease in the live cell count and increase in the dead cell count show that a certain proportion of live cells are getting killed due to the flow. Figure 7 illustrates the proportions of live and dead cells on the nanostructured surface and those remaining after the flow.

As seen from the results on dead cells on the nanostructured surface,

$D_0 < D_1$ , and since no new cells were introduced to the surface,

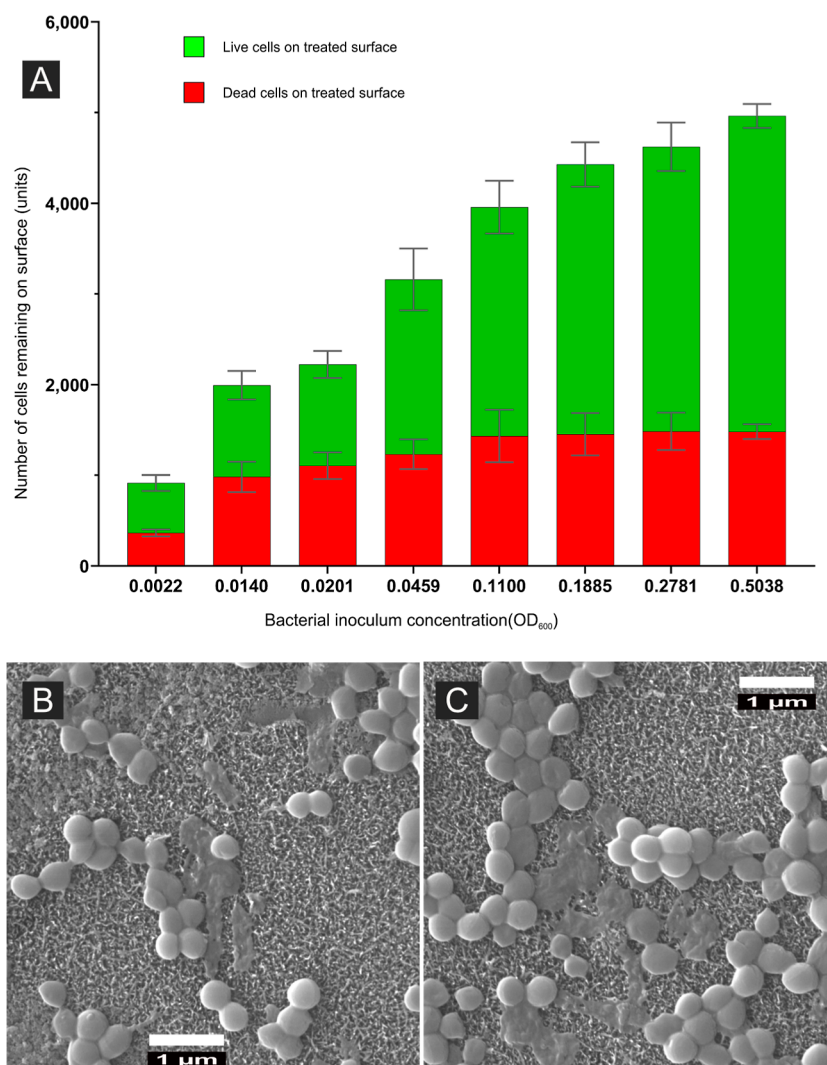


**Figure 6.** (A) Live and dead cell count on the nanostructured surface with different inoculum concentrations. Eight suspensions of *S. aureus* were prepared with varying cell concentrations, and the substrate was placed in 1 mL of each suspension. Following 20 min incubation at 37 °C, substrates were taken out of the bacterial suspension without rinsing them and stained with SYTO9 and PI before imaging using a fluorescence microscope. The adherent cell count was quantified by measuring the surface coverage with pixel counting of the image. Compared to the lowest-concentration cell count, all cell counts (both live and dead) were significantly increased, and the live cell count of second and third lowest concentrations was measured with Student's *t*-test. (B) SEM image of *S. aureus* cells with the lowest concentration (OD<sub>600</sub> = 0.0022) on the treated surface. (C) SEM images of *S. aureus* cells with the highest cell concentration (OD<sub>600</sub> = 0.5038) on the treated surface.

$$D_1 = D_0 - D_R + K_{0-1}$$

$$\therefore D_0 < D_0 - D_R + K_{0-1}$$

$\therefore D_R < K_{0-1} \rightarrow$  The number of cells getting killed during the flow is greater than the number of dead cells removed from the surface.

Similarly, as seen from Results,  $L_0 > L_1$  and  $L_0 = L_1 + L_R + K_{0-1}$

$$\therefore L_0 > L_0 - L_R - K_{0-1}$$

$\therefore 0 < L_R + K_{0-1} \rightarrow$  The sum of the number of live cells detached from the surface and the number of cells killed during the flow is positive.

$$\Delta D = K_{0-1} - D_R > 0$$

$$\Delta L = K_{0-1} + L_R > 0$$

$$\therefore 0 < D_R < K_{0-1} < (K_{0-1} + L_R) < L_0$$

where  $D_0$  is the number of dead cells on the surface before the flow,  $L_0$  is the number of live cells on the surface before the flow,  $D_1$  is the number of dead cells remaining on the surface after flow,  $L_1$  is the number of live cells remaining on the surface after the flow,  $D_R$  is the number of dead cells removed from the surface during the flow,  $L_R$  is the number of live cells removed from the surface during the flow, and  $K_{0-1}$  is the number of cells killed during the flow.

Cell death on nanotopographic surfaces under flow conditions was significantly increased for both species of bacteria tested. Analysis of results showed that a certain number of live cells were lysed during the flow (as  $K_{0-1} > 0$ ). This can be due to the effect of hydrodynamic forces exerted by the flow on cells which causes cells to collide with nanowires on the surface, resulting in an increase in the number of dead cells on the surface. This phenomenon is reported in the literature as well.<sup>11</sup> Furthermore, the number of live cells lysed during the flow is higher than the number of



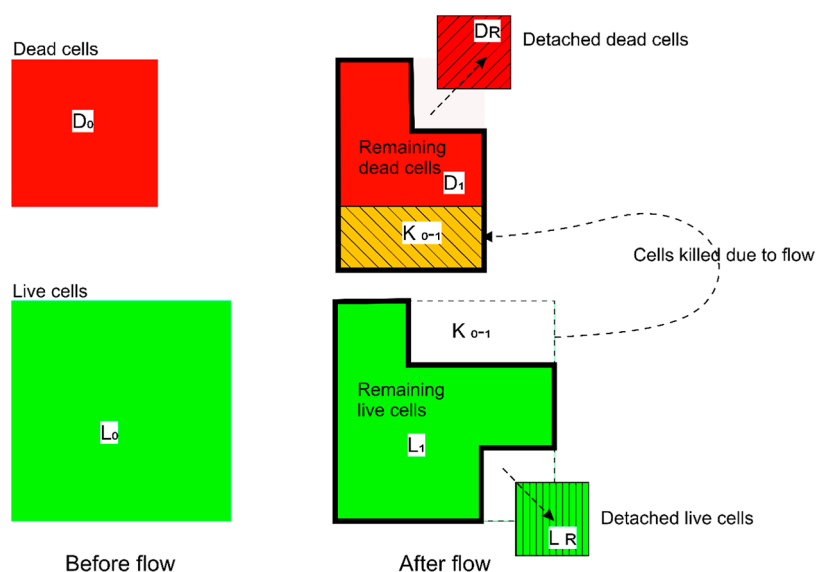


**Figure 7.** Schematic illustration of proportions of live and dead cells on the nanostructured surface before and after flow.  $D_0$  and  $L_0$  represent the amount of dead and live cells on the surface, respectively. Cell counts from the no-flow experiment show that the number of live cells is greater than the number of dead cells. During rinsing flow, the  $L_R$  number of live cells was removed from the surface, as suggested by the reduction in the cell count after the flow. However, according to the results, the number of dead cells was increased after rinsing. Moreover, a certain number of dead cells ( $D_R$ ) can be expected to be removed from the surface. This suggests that a number of live cells have been killed in addition to getting removed from the surface. The number of cells killed ( $K_{0-1}$ ) must be greater than the number of dead cells advected by the flow.

dead cells removed from the surface. However, there is a considerable difference in the dead cell count with the increasing flowrate for the two species. Dead cell counts under no flow and 10 mL/min flow were not significantly different for *P. aeruginosa*, and it increased at 50 mL/min flow, but the same is not significantly different between 50 and 100 mL/min flows. Dead cell counts of *S. aureus* increased from no-flow to all-flow conditions significantly, but there was no significant difference with increasing flow. This can be due to the differential effect of hydrodynamic forces on cells. Comparatively, *P. aeruginosa* cells are bigger in size than *S. aureus* cells. Therefore, the smaller *S. aureus* cells which are spherical also experience lesser drag by the flow, resulting in lesser collisions with nanofeatures on the surface compared to *P. aeruginosa*. Moreover, *P. aeruginosa* on metal surfaces had an adhesion strength of 95 pN<sup>56</sup> and that of *S. aureus* on metal surfaces was 11 nN,<sup>57</sup> which is approximately 1,100 times the adhesion strength of *P. aeruginosa*. Higher drag force and lesser adhesion strength of *P. aeruginosa* may have caused the cells to detach from the surface more easily. This is reflected by 38% reduction of *P. aeruginosa* cells from no flow to flow, while *S. aureus* had a reduction of only 19%. Furthermore, reduction in *P. aeruginosa* cells from the nanostructured surface was statistically significant until the flowrate is increased to 50 mL/min, but with *S. aureus*, reduction in the cell count was not significant above the 10 mL/min flowrate. This again confirms that flow is more effective on *P. aeruginosa* species.

The inspirations for developing artificial bactericidal nanostructured surfaces were the natural bactericidal nanotopographic surfaces such as cicada wings<sup>1</sup> and dragonfly wings.<sup>4</sup> These natural surfaces do have a self-cleaning ability;<sup>1,58–61</sup> however, our results show that the biomimetic artificial bactericidal nanotopographic surfaces cannot be cleaned with a flow of a fluid. Most of the exemplar natural surfaces do have the advantages in terms of self-cleaning ability. Hydrophobicity of the surfaces is regarded as a key property that determines

the self-cleaning ability of the surface by preventing adhesions.<sup>58,62,63</sup> However, removal of adherent cells requires a mechanism. Unlike the artificial nanostructures, these natural nanostructures are comparatively less stiff.<sup>42,64</sup> Surfaces, such as dragonfly or cicada wings, are flapped at an extremely high rate; therefore, adherent cells are subjected to centrifugal forces acting on them. Any of the above-mentioned advantages are not available for the biomimetic artificial surfaces. Unavailability of such a self-cleaning mechanism would create a great challenge for the next generation of bactericidal nanostructured surfaces translating into real-world applications. Our results show that irrespective of the number of cells coming in contact with the nanostructured surface, it can lyse a limited number of bacterial cells. Therefore, once the surface is saturated with lysed cells, it cannot kill cells further.

Testing nanotopographic surfaces for bactericidal efficacy is done by adopted methods of an ISO standard developed for testing antimicrobial coatings. These methods are slightly varied among researchers, but rinsing of the bacterium-incubated substrate before quantifying the live and dead cells on the surface is a common step. Our results show that substrates subjected to fluid flow cause disproportionate removal of live and dead cells from the surface. Therefore, rinsing of the substrate can lead to exaggerated bactericidal efficacy as more live cells are removed by the flow. This necessitates a standard protocol for testing nanotopographic antibacterial surfaces.

## CONCLUSIONS

Fluid flow causes a significant detachment of adherent cells from nanostructured surfaces. However, the reduction in the cell count is not flowrate-dependent. It is evident that the detachment of dead cells from the surface is drastically different from live cell detachment. Flow causes the number of dead cells on the surface to increase, but it is independent of the flowrate. However, a reduction of live cells resulted from

the flow, and it is flowrate-dependent. A nanostructured surface can kill only a certain number of bacterial cells encountering it. After reaching a saturation dead cell count, nanostructured surfaces cannot kill cells any further.

## ■ ASSOCIATED CONTENT

### SI Supporting Information

The Supporting Information is available free of charge at <https://pubs.acs.org/doi/10.1021/acsomega.2c01208>.

Live to dead cell ratios of *P. aeruginosa* and *S. aureus* on treated and untreated surfaces under the four different flow conditions tested, comparison of cell numbers between *P. aeruginosa* and *S. aureus* cells on treated and untreated surfaces under the four different flow conditions tested, and *S. aureus* cell count on treated surfaces with cell concentrations incubated under static conditions (and without rinsing) for 20 min (PDF)

## ■ AUTHOR INFORMATION

### Corresponding Author

Prasad K. D. V. Yarlagadda – Centre for Biomedical Technologies, Queensland University of Technology, Brisbane, QLD 4000, Australia; School of Mechanical, Medical, and Process Engineering, Faculty of Engineering, Queensland University of Technology, Brisbane 4000 QLD, Australia; [orcid.org/0000-0002-7026-4795](https://orcid.org/0000-0002-7026-4795); Email: [y.prasad@qut.edu.au](mailto:y.prasad@qut.edu.au)

### Authors

S. W. M. A. Ishantha Senevirathne – Centre for Biomedical Technologies, Queensland University of Technology, Brisbane, QLD 4000, Australia; School of Mechanical, Medical, and Process Engineering, Faculty of Engineering, Queensland University of Technology, Brisbane 4000 QLD, Australia; [orcid.org/0000-0002-7746-7069](https://orcid.org/0000-0002-7746-7069)

Yi-Chin Toh – Centre for Biomedical Technologies, Queensland University of Technology, Brisbane, QLD 4000, Australia; School of Mechanical, Medical, and Process Engineering, Faculty of Engineering, Queensland University of Technology, Brisbane 4000 QLD, Australia; [orcid.org/0000-0002-4105-4852](https://orcid.org/0000-0002-4105-4852)

Complete contact information is available at: <https://pubs.acs.org/10.1021/acsomega.2c01208>

### Notes

The authors declare no competing financial interest.

## ■ ACKNOWLEDGMENTS

Authors wish to acknowledge support from following individuals and institutions: the Centre for Biomedical Technologies (CBT), Queensland University of Technology (QUT), Australia, Dr. K.A.S.N. Gunarathne for support in designing experiments with microbes, Dr. Phong Tran for inspirations in writing the manuscript, and Dr. Christina Theodoropoulos for support for fluorescence microscopy. The first author is a lecturer from the University of Moratuwa, Sri Lanka, currently attached to QUT. Funding was received for this work from the AHEAD project (Grant: AHEAD/PhD/R2/ENG/TECH/161), University Grants Commission of Sri Lanka.

## ■ REFERENCES

- (1) Ivanova, E. P.; Hasan, J.; Webb, H. K.; Truong, V. K.; Watson, G. S.; Watson, J. A.; Baulin, V. A.; Pogodin, S.; Wang, J. Y.; Tobin, M. J.; Löbbe, C.; Crawford, R. J. Natural Bactericidal Surfaces: Mechanical Rupture of *Pseudomonas Aeruginosa* Cells by Cicada Wings. *Small* **2012**, *8*, 2489–2494.
- (2) Pogodin, S.; Hasan, J.; Baulin, V. A.; Webb, H. K.; Truong, V. K.; Phong Nguyen, T. H.; Boshkovikj, V.; Fluke, C. J.; Watson, G. S.; Watson, J. A.; Crawford, R. J.; Ivanova, E. P. Biophysical Model of Bacterial Cell Interactions with Nanopatterned Cicada Wing Surfaces. *Biophys. J.* **2013**, *104*, 835–840.
- (3) Hasan, J.; Webb, H. K.; Truong, V. K.; Pogodin, S.; Baulin, V. A.; Watson, G. S.; Watson, J. A.; Crawford, R. J.; Ivanova, E. P. Selective Bactericidal Activity of Nanopatterned Superhydrophobic Cicada *Psaltoda Claripennis* Wing Surfaces. *Appl. Microbiol. Biotechnol.* **2013**, *97*, 9257–9262.
- (4) Bandara, C. D.; Singh, S.; Afara, I. O.; Wolff, A.; Tesfamichael, T.; Ostrikov, K.; Oloyede, A. Bactericidal Effects of Natural Nanotopography of Dragonfly Wing on *Escherichia Coli*. *ACS Appl. Mater. Interfaces* **2017**, *9*, 6746–6760.
- (5) Ishantha Senevirathne, S. W. M. A.; Hasan, J.; Mathew, A.; Jaggesar, A.; Yarlagadda, P. K. D. V. Trends in Bactericidal Nanostructured Surfaces: An Analytical Perspective. *Appl. Bio Mater.* **2021**, *4*, 7626 acsabm.
- (6) Velic, A.; Hasan, J.; Li, Z.; Yarlagadda, P. K. D. V. Mechanics of Bacterial Interaction and Death on Nanopatterned Surfaces. *Biophys. J.* **2021**, *120*, 217–231.
- (7) Wu, S.; Zuber, F.; Maniura-Weber, K.; Brugger, J.; Ren, Q. Nanostructured Surface Topographies Have an Effect on Bactericidal Activity. *J. Nanobiotechnol.* **2018**, *16*, 1–9.
- (8) Michalska, M.; Gambacorta, F.; Divan, R.; Aranson, I. S.; Sokolov, A.; Noirot, P.; Laible, P. D. Tuning Antimicrobial Properties of Biomimetic Nanopatterned Surfaces. *Nanoscale* **2018**, *10*, 6639–6650.
- (9) Lai, C. Q. Bacterial Attachment, Aggregation, and Alignment on Subcellular Nanogratings. *Langmuir* **2018**, *34*, 4059–4070.
- (10) Modaresifar, K.; Azizian, S.; Ganjian, M.; Fratila-Apachitei, L. E.; Zadpoor, A. A. Bactericidal Effects of Nanopatterns: A Systematic Review. *Acta Biomater.* **2019**, *83*, 29–36.
- (11) Li, L.; Tian, F.; Chang, H.; Zhang, J.; Wang, C.; Rao, W.; Hu, H. Interactions of Bacteria With Monolithic Lateral Silicon Nanospikes Inside a Microfluidic Channel. *Front. Chem.* **2019**, *7*, 1–8.
- (12) Senevirathne, S. W. M. A. I.; Hasan, J.; Mathew, A.; Woodruff, M.; Yarlagadda, P. K. D. V. Bactericidal Efficiency of Micro- and Nanostructured Surfaces: A Critical Perspective. *RSC Adv.* **2021**, *11*, 1883–1900.
- (13) Xie, Y.; Chen, S.; Peng, X.; Wang, X.; Wei, Z.; Richardson, J. J.; Liang, K.; Ejima, H.; Guo, J.; Zhao, C. Bioactive Materials Alloyed Nanostructures Integrated Metal-Phenolic Nanopatform for Synergistic Wound Disinfection and Revascularization. *Bioact. Mater.* **2022**, *16*, 95–106.
- (14) Isa, N. N. C.; Mohd, Y.; Mohamad, S.A. S.; Zaki, M. H. M. Physicochemical Properties and Antibacterial Activity of Nanostructured Copper Electrodeposited on Stainless Steel Surface. *Malays. J. Biochem. Mol. Biol.* **2022**, *24*, 1–10.
- (15) Yi, Y.; Jiang, R.; Liu, Z.; Dou, H.; Song, L.; Tian, L.; Ming, W.; Ren, L.; Zhao, J. Bioinspired Nanopillar Surface for Switchable Mechano-Bactericidal and Releasing Actions. *J. Hazard. Mater.* **2022**, *432*, 128685.
- (16) Hasan, J.; Pyke, A.; Nair, N.; Yarlagadda, T.; Will, G.; Spann, K.; Yarlagadda, P. K. D. V. Antiviral Nanostructured Surfaces Reduce the Viability of SARS-CoV-2. *ACS Biomater. Sci. Eng.* **2020**, *6*, 4858–4861.
- (17) Hasan, J.; Jain, S.; Chatterjee, K. Nanoscale Topography on Black Titanium Imparts Multi-Biofunctional Properties for Orthopedic Applications. *Sci. Rep.* **2017**, *7*, 1–13.
- (18) Hasan, J.; Jain, S.; Padmarajan, R.; Purighalla, S.; Sambandamurthy, V. K.; Chatterjee, K. Multi-Scale Surface Top-

- ography to Minimize Adherence and Viability of Nosocomial Drug-Resistant Bacteria. *Mater. Des.* **2018**, *140*, 332–344.
- (19) Viela, F.; Navarro-Baena, I.; Jacobo-Martín, A.; Hernández, J. J.; Boyano-Escalera, M.; Osorio, M. R.; Rodríguez, I. Nano-Engineering Safer-by-Design Nanoparticle Based Moth-Eye Mimetic Bactericidal and Cytocompatible Polymer Surfaces. *RSC Adv.* **2018**, *8*, 22606–22616.
- (20) Linklater, D. P.; Juodkazis, S.; Crawford, R. J.; Ivanova, E. P. Mechanical Inactivation of Staphylococcus Aureus and Pseudomonas Aeruginosa by Titanium Substrata with Hierarchical Surface Structures. *Materialia* **2019**, *5*, 100197.
- (21) Jindai, K.; Nakade, K.; Masuda, K.; Sagawa, T.; Kojima, H.; Shimizu, T.; Shingubara, S.; Ito, T. Adhesion and Bactericidal Properties of Nanostructured Surfaces Dependent on Bacterial Motility. *RSC Adv.* **2020**, *10*, 5673–5680.
- (22) ISO. ISO 22196:2011. *Measurement of Antibacterial Activity on Plastics and Other Non-Porous Surfaces*; BSI, .
- (23) Liu, Z.; Zhang, K.; Cheng, X. Rheology of Bacterial Suspensions under Confinement. *Rheol. Acta* **2019**, *58*, 439–451.
- (24) Kaya, T.; Koser, H. Direct Upstream Motility in Escherichia Coli. *Biophys. J.* **2012**, *102*, 1514–1523.
- (25) Hill, J.; Kalkanci, O.; McMurry, J. L.; Koser, H. Hydrodynamic Surface Interactions Enable Escherichia Coli to Seek Efficient Routes to Swim Upstream. *Phys. Rev. Lett.* **2007**, *98*, 1–4.
- (26) Rosenzweig, R.; Perinbam, K.; Ly, V. K.; Ahrar, S.; Siryaporn, A.; Yee, A. F. Nanopillared Surfaces Disrupt Pseudomonas Aeruginosa Mechanoresponsive Upstream Motility. *ACS Appl. Mater. Interfaces* **2019**, *11*, 10532–10539.
- (27) Liu, Y.; Tay, J.-H. Metabolic Response of Biofilm to Shear Stress in Fixed-Film Culture. *J. Appl. Microbiol.* **2001**, *90*, 337–342.
- (28) Foka, A.; Katsikogianni, M. G.; Katsikogianni, M.; Anastassiou, E.; Spiliopoulou, I.; Missirlis, Y. The Combined Effect of Surface Chemistry and Flow Conditions on Staphylococcus Epidermidis Adhesion and Ica Operon Expression. *Eur. Cells Mater.* **2012**, *24*, 386–402.
- (29) Hizal, F.; Choi, C.-H.; Busscher, H. J.; van der Mei, H. C. Staphylococcal Adhesion, Detachment and Transmission on Nanopillared Si Surfaces. *ACS Appl. Mater. Interfaces* **2016**, *8*, 30430–30439.
- (30) Arpa-Sancet, M. P.; Christophis, C.; Rosenhahn, A. Microfluidic Assay to Quantify the Adhesion of Marine Bacteria. *Biointerphases* **2012**, *7*, 26.
- (31) Hizal, F.; Rungraeng, N.; Lee, J.; Jun, S.; Busscher, H. J.; van der Mei, H. C.; Choi, C.-H. Nanoengineered Superhydrophobic Surfaces of Aluminum with Extremely Low Bacterial Adhesivity. *ACS Appl. Mater. Interfaces* **2017**, *9*, 12118–12129.
- (32) Thomen, P.; Robert, J.; Monmeyran, A.; Bitbol, A.-F.; Douarache, C.; Henry, N. Bacterial Biofilm under Flow: First a Physical Struggle to Stay, Then a Matter of Breathing. *PLoS One* **2017**, *12*, No. e0175197.
- (33) Liu, Y.; Tay, J.-H. The Essential Role of Hydrodynamic Shear Force in the Formation of Biofilm and Granular Sludge. *Water Res.* **2002**, *36*, 1653–1665.
- (34) CHRISTERSSON, C. E.; GLANTZ, P.-O. J.; BAIER, R. E. Role of Temperature and Shear Forces on Microbial Detachment. *Eur. J. Oral Sci.* **1988**, *96*, 91–98.
- (35) Yang, J.; Shimogonya, Y.; Ishikawa, T. Bacterial Detachment from a Wall with a Bump Line. *Phys. Rev. E* **2019**, *99*, 1–8.
- (36) Sjollem, J.; Van Der Mei, H. C.; Hall, C. L.; Peterson, B. W.; De Vries, J.; Song, L.; Jong, E. D. D.; Busscher, H. J.; Swartjes, J. J. T. M. Detachment and Successive Re-Attachment of Multiple, Reversibly-Binding Tethers Result in Irreversible Bacterial Adhesion to Surfaces. *Sci. Rep.* **2017**, *7*, 1–13.
- (37) Gómez-Suárez, C.; Busscher, H. J.; Van Der Mei, H. C. Analysis of Bacterial Detachment from Substratum Surfaces by the Passage of Air-Liquid Interfaces. *Appl. Environ. Microbiol.* **2001**, *67*, 2531–2537.
- (38) Emmert, S.; Davis, K.; Gerlach, R.; Class, H. The Role of Retardation, Attachment and Detachment Processes during Microbial Coal-Bed Methane Production after Organic Amendment. *Water* **2020**, *12*, 3008–25.
- (39) Busscher, H. J.; Van Der Mei, H. C. Microbial Adhesion in Flow Displacement Systems. *Clin. Microbiol. Rev.* **2006**, *19*, 127–141.
- (40) Nejadnik, M. R.; Van Der Mei, H. C.; Busscher, H. J.; Norde, W. Determination of the Shear Force at the Balance between Bacterial Attachment and Detachment in Weak-Adherence Systems, Using a Flow Displacement Chamber. *Appl. Environ. Microbiol.* **2008**, *74*, 916–919.
- (41) Krsmanovic, M.; Biswas, D.; Ali, H.; Kumar, A.; Ghosh, R.; Dickerson, A. K. Hydrodynamics and Surface Properties Influence Biofilm Proliferation. *Adv. Colloid Interface Sci.* **2021**, *288*, 102336.
- (42) Siddiqui, S.; Chandrasekaran, A.; Lin, N.; Tufenkji, N.; Moraes, C. Microfluidic Shear Assay to Distinguish between Bacterial Adhesion and Attachment Strength on Stiffness-Tunable Silicone Substrates. *Langmuir* **2019**, *35*, 8840–8849.
- (43) Tripathy, A.; Sen, P.; Su, B.; Briscoe, W. H. Natural and Bioinspired Nanostructured Bactericidal Surfaces. *Adv. Colloid Interface Sci.* **2017**, *248*, 85–104.
- (44) van Loosdrecht, M. C.; Lyklema, J.; Norde, W.; Zehnder, A. J. J. Bacterial Adhesion: A Physicochemical Approach. *Microb. Ecol.* **1989**, *17*, 1–15.
- (45) Cheng, Y.; Feng, G.; Moraru, C. I. Micro- and Nanotopography Sensitive Bacterial Attachment Mechanisms: A Review. *Front. Microbiol.* **2019**, *10*, 1–17.
- (46) Absolom, D. R.; Lamberti, F. V.; Policova, Z.; Zingg, W.; van Oss, C. J.; Neumann, A. W. Surface Thermodynamics of Bacterial Adhesion. *Appl. Environ. Microbiol.* **1983**, *46*, 90–97.
- (47) Sanfilippo, J. E.; Lorestani, A.; Koch, M. D.; Bratton, B. P.; Siryaporn, A.; Stone, H. A.; Gitai, Z. Microfluidic-Based Transcriptomics Reveal Force-Independent Bacterial Rheosensing. *Nat. Microbiol.* **2019**, *4*, 1274–1281.
- (48) Misra, G.; Rojas, E. R.; Gopinathan, A.; Huang, K. C. Mechanical Consequences of Cell-Wall Turnover in the Elongation of a Gram-Positive Bacterium. *Biophys. J.* **2013**, *104*, 2342–2352.
- (49) Cai, Q.; Li, Z.; Ouyang, Q.; Luo, C.; Gordon, V. D. Singly Flagellated Pseudomonas Aeruginosa Chemotaxes Efficiently by Unbiased Motor Regulation. *MBio* **2016**, *7*, 1–9.
- (50) Tan, J.; Zhou, B.; Luo, Y.; Karwe, M. V. Numerical Simulation and Experimental Validation of Bacterial Detachment Using a Spherical Produce Model in an Industrial-Scale Flume Washer. *Food Control* **2021**, *130*, 108300.
- (51) Jaggessar, A.; Tesfamichael, T.; Wang, H.; Yan, C.; Yarlagadda, P. K. D. V. Investigation of Mechanical Properties and Morphology of Hydrothermally Manufactured Titanium Dioxide Nanostructured Surfaces. *Procedia Manuf.* **2019**, *30*, 373–379.
- (52) Bright, R.; Hayles, A.; Wood, J.; Ninan, N.; Palms, D.; Visalakshan, R. M.; Burzava, A.; Brown, T.; Barker, D.; Vasilev, K. Bio-Inspired Nanostructured Ti-6Al-4V Alloy: The Role of Two Alkaline Etchants and the Hydrothermal Processing Duration on Antibacterial Activity. *Nanomater.* **2022**, *12*, 1140.
- (53) Jaggessar, A.; Mathew, A.; Tesfamichael, T.; Wang, H.; Yan, C.; Yarlagadda, P. K. Bacteria Death and Osteoblast Metabolic Activity Correlated to Hydrothermally Synthesised TiO<sub>2</sub> Surface Properties. *Molecules* **2019**, *24*, 1201.
- (54) Jaggessar, A.; Yarlagadda, P. K. D. V. Modelling the Growth of Hydrothermally Synthesised Bactericidal Nanostructures, as a Function of Processing Conditions. *Mater. Sci. Eng. Carbon* **2020**, *108*, 110434.
- (55) Bogachev, M. I.; Volkov, V. Y.; Markelov, O. A.; Trizna, E. Y.; Baydamshina, D. R.; Melnikov, V.; Murtazina, R. R.; Zelenikhin, P. V.; Sharafutdinov, I. S.; Kayumov, A. R. Fast and Simple Tool for the Quantification of Biofilm-Embedded Cells Sub-Populations from Fluorescent Microscopic Images. *PLoS One* **2018**, *13*, e0193267–24.
- (56) Touhami, A.; Jericho, M. H.; Boyd, J. M.; Beveridge, T. J. Nanoscale Characterization and Determination of Adhesion Forces of Pseudomonas Aeruginosa Pili by Using Atomic Force Microscopy. *J. Bacteriol.* **2006**, *188*, 370–377.

(57) Alam, F.; Balani, K. Adhesion Force of Staphylococcus Aureus on Various Biomaterial Surfaces. *J. Mech. Behav. Biomed. Mater.* **2017**, *65*, 872–880.

(58) Bhushan, B.; Jung, Y. C. Natural and Biomimetic Artificial Surfaces for Superhydrophobicity, Self-Cleaning, Low Adhesion, and Drag Reduction. *Prog. Mater. Sci.* **2011**, *56*, 1–108.

(59) Bixler, G. D. Ph.D. Thesis, Bioinspired Surface for Low Drag, Self-Cleaning, and Antifouling: Shark Skin, Butterfly and Rice Leaf Effects, The Ohio State University, 2013; Vol. 1.

(60) Jaggessar, A.; Shahali, H.; Mathew, A.; Yarlaga, P. K. D. V. Bio-Mimicking Nano and Micro-Structured Surface Fabrication for Antibacterial Properties in Medical Implants. *J. Nanobiotechnol.* **2017**, *15*, 1–20.

(61) Webb, H. K.; Crawford, R. J.; Ivanova, E. P. Introduction to Antibacterial Surfaces. In *Antibacterial Surfaces*; Ivanova, E. P., Crawford, R. J., Eds.; 2015; pp 1–8.

(62) Watson, G. S.; Green, D. W.; Schwarzkopf, L.; Li, X.; Cribb, B. W.; Myhra, S.; Watson, J. A. A Gecko Skin Micro/Nano Structure - A Low Adhesion, Superhydrophobic, Anti-Wetting, Self-Cleaning, Biocompatible, Antibacterial Surface. *Acta Biomater.* **2015**, *21*, 109–122.

(63) Hasan, J.; Raj, S.; Yadav, L.; Chatterjee, K. Engineering a Nanostructured “Super Surface” with Superhydrophobic and Superkilling Properties. *RSC Adv.* **2015**, *5*, 44953–44959.

(64) Bandara, C. D. Ph.D. Thesis, Characterisation of The Bactericidal Efficacy of Natural Nano-Topography Using Dragonfly Wing as a Model, Queensland University of Technology, 2017.